

Research Article

Arwa Althomali, Maha H. Daghestani, Fatimah Basil Almukaynizi, Sabah Ahmed Al-Zahrani, Manal A. Awad, Nada M. Merghani, Wadha I. Bukhari, Eiman M. Ibrahim, Sherifah M. Alzahrani, Nouf Altowair, Afaf S. AL-Ghamdi, Asma M. AlQahtani, Rasha Ramadan, and Ramesa Shafi Bhat*

Anti-colon cancer activities of green-synthesized *Moringa oleifera*–AgNPs against human colon cancer cells

<https://doi.org/10.1515/gps-2022-0052>

received March 03, 2022; accepted April 20, 2022

Abstract: The anticancer activity of silver nanoparticles (AgNPs) is well known to be synthesized using green-synthesized methods, although its mechanism of action is not understood fully. *Moringa oleifera* leaves were used as reducing and stabilizing agents to synthesize AgNPs. Green-synthesized AgNPs were characterized using ultraviolet-visible spectroscopy, dynamic light scattering, transmission electronic microscopy, scanning electronic microscopy, Fourier transform infrared, and energy-dispersive X-ray spectroscopy analyses. The synthesized nanoparticles were then characterized by their anticancer properties by performing a 3-(4,5-dimethylthiazol-2-yl)-2,5-diphenyltetrazolium bromide assay. The real-time

polymerase chain reaction was used to check the expression levels of the four genes (β -catenin, adenomatous polyposis coli (*APC*), and lipoprotein receptor-related proteins 5 and 6 (*LRP5/6*)). The synthesized nanoparticles were 25 nm on average and spherical in shape and aggregated form. Noteworthy cytotoxicity is how green-synthesized *M. oleifera*–AgNPs were observed in comparison with the *M. oleifera* leaf extract against a cancerous cell line. The *M. oleifera*–AgNPs decreased the expression of *CTNNB1* and *LRP6* genes, while the *LRP5* gene expression increased in both cell lines. With treatment, the *APC* gene expression decreased in SW480 but increased in HTC116. Our results imply that AgNPs synthesized by *M. oleifera* extract could be an ideal strategy to combat colon cancer.

Keywords: *Moringa oleifera*, plant extract, nanosilver, anticancer activity

* **Corresponding author: Ramesa Shafi Bhat**, Biochemistry Department, College of Science, King Saud University, PO Box 22452, Riyadh 11495, Saudi Arabia, e-mail: rbhat@ksu.edu.sa

Arwa Althomali, Fatimah Basil Almukaynizi: Prince Naif Bin Abdul Aziz Health Research Center, King Saud University, Riyadh, Saudi Arabia

Maha H. Daghestani: Department of Zoology, College of Science, Centre for Scientific and Medical Female Colleges, King Saud University, Riyadh, Saudi Arabia

Sabah Ahmed Al-Zahrani: Biochemistry Department, College of Science, King Saud University, PO Box 22452, Riyadh 11495, Saudi Arabia

Manal A. Awad: King Abdullah Institute for Nanotechnology, King Saud University, Riyadh 11451, Saudi Arabia

Nada M. Merghani, Wadha I. Bukhari, Eiman M. Ibrahim, Sherifah M. Alzahrani, Nouf Altowair, Afaf S. AL-Ghamdi,

Asma M. AlQahtani, Rasha Ramadan: Central Research Laboratory, Female Center for Medical Studies and Scientific Section, King Saud University, Riyadh, Saudi Arabia

1 Introduction

Silver ions have been used in medicine historically, although silver nanoparticles (AgNPs) offer more possibilities for use in many types of medical treatments for humans [1]. AgNPs are the most widely used particles among metallic nanoparticles, accounting for almost 25% [2]. AgNPs are being incorporated into many surgical instruments daily, such as in face masks and even in bone-cementing materials, for their excellent antibacterial, antifungal, and antiviral properties [3,4]. Indeed, AgNPs are replacing silver sulfadiazine for wound-healing treatments [4,5]. Chemical methods produce AgNPs, but the reagents used in these processes usually are expensive and toxic to humans [6].

In recent tests of biological sources such as plants, seaweeds, insects, and microorganisms, silver ions were successfully reduced to AgNPs by reducing the capacities

of the metabolites present in them [7–11]. AgNP synthesis via plant extract is better than other biological extracts in terms of availability, low toxicity, and the presence of rich phytochemicals such as alkaloids, flavonoids, flavones, terpenoids, terpenes, polysaccharides, phenolics, saponins, and tannins [12]. In addition, plant extracts are reducing and stabilizing agents during the AgNP synthesis process. The AgNPs synthesized through biologic approaches maintain a homogenous chemical composition and show promising results against many cancer cell lines [13]. Therefore, green-synthesis methods based on green chemistry offer an alternative to the chemical and physical synthesis of AgNPs used for anticancer treatments [7].

Although many studies have reported on the anti-tumor properties of AgNPs, their mechanism of action is not fully understood. The cytotoxicity of green-synthesized AgNPs depends on their size and shape: those synthesized from plant sources are usually spherical and cytotoxic against many human cancer cell lines [14]. Due to their small size, AgNPs can directly contact cell surfaces to initiate DNA damage and change the gene expression, which may result in cell death [14,15].

Colorectal cancer (CRC) was the second deadliest and third most common malignant tumor worldwide in 2020 [16]. The occurrence of this disease is much higher in Saudi Arabia as it is at the topmost in men and the third in females [17]. In this study, we investigated the cytotoxicity of AgNPs synthesized via aqueous extracts from *Moringa oleifera* leaves against two human colon cancer cell lines, SW480 and HTC116.

2 Materials and methods

2.1 Chemicals

The chemicals used and the manufacturer details are as follows: silver nitrate: Fisher chemical – Lot 1214151; trypsin: Sigma 5942C; phosphate-buffered saline (PBS): Sigma P5368-10PAK; 3-(4,5-dimethylthiazol-2-yl)-2,5-diphenyltetrazolium bromide (MTT): Sigma Aldrich, UK; dimethyl sulfoxide solution (DMSO): Ajax Finechem Pty Ltd, Australia; Minimum Essential Medium: Stem Cell Technologies Cat# 36453.

2.2 *M. oleifera* leaf extract

Fresh *M. oleifera* leaves that were cultivated in the Riyadh region of Saudi Arabia were included in this study. Taxonomic identification of *M. oleifera* was confirmed by Dr. Mona S. Alwhibi in the Botany and Microbiology Department, College of Science, King Saud University. Fifteen grams of fresh leaves were boiled in 150 mL of distilled water (1:10 weight/volume ratio) for 20 min. After cooling, the extract was filtered. The collected filtrate was used for the green synthesis of AgNPs.

2.3 Preparation of green-synthesized *M. oleifera*-AgNPs

Freshly prepared leaf extract was mixed with a silver nitrate solution, with a final concentration of 5 mM. The mixture was incubated at room temperature until a reduction of silver ions to AgNPs was observed based on color change. The preparation of AgNPs was confirmed by ultraviolet (UV)-visible (vis) spectrophotometer by measuring the absorbance of the mixture, from 300 to 600 nm.

2.4 Characterization of green-synthesized *M. oleifera*-AgNPs

At first, the green synthesis of *M. oleifera*-AgNPs was achieved by monitoring the color change, from green to brown, followed by recording the absorbance peak, from 300 to 600 nm. Then, the average size of the *M. oleifera*-AgNPs was recorded by analyzing the zeta potential and using transmission electron microscopy (TEM) and scanning electron microscopy (SEM). By bioreducing the functional groups of *M. oleifera* leaves, the extracts were recorded using infrared spectroscopy. Energy-dispersive X-ray spectroscopy validated the presence of specific elements in the sample.

2.5 Cell culture

The human colon cancer cell lines, HTC116 and SW480, were cultured in Eagle minimum essential medium under

a humidified incubator with 5% CO₂. Trypsin was used to harvest the cells, followed by washing in PBS, and then was used for further experiments.

2.6 Cytotoxic activity of green-synthesized *M. oleifera*-AgNPs

Cancer cells were seeded in a 96-well plate at a density of 2×10^5 cells·well⁻¹ in 100 µL optimized medium, grown to a density of 2×10^4 cells·well⁻¹ for 24 h, and then exposed to various test concentrations of digitate extract and green-synthesized digitate-AgNPs separately for 48 h. Finally, 100 µL of MTT was added at 37°C at a final concentration of 5 mg·mL⁻¹. The 96-well plate was kept in the dark for 2 h before the medium-containing MTT was removed. About 100 µL of DMSO was added to dissolve the formazane crystals. The 96-well plate was also shaken in the dark for 15 min, to help dissolve the formazane crystals. The optical density of each treatment was measured at a 490 nm absorbance, using a 96-well plate reader (Molecular Devices, SPECTRA max, PLUS384). Each experiment was performed in four replicates. The values of the optical densities were normalized according to the control (untreated cells).

2.7 Gene-expression analysis

Gene-expression analysis was performed after treating the cells with IC₅₀ of green-synthesized *M. oleifera*-AgNPs and *M. oleifera* extract separately. The cells were incubated for 24 h and then harvested for RNA extraction.

2.8 RNA isolation and real-time polymerase chain reaction (RT-PCR)

An RT-PCR was performed using the High-Capacity cDNA Reverse Transcription Kit (Applied Biosystems, Foster City, CA, USA). The cDNA was stored at -20°C until the RT-PCR experiment was conducted. The GAPDH gene was used as an internal control. The oligonucleotide sequences are listed in Table 1. The RT-PCR was done on a LightCycler ViiA 7 Instrument (ViiA 7, Thermo Fisher Scientific). The data were obtained using LightCycler ViiA 7 software 1.0 (ViiA 7, Thermo Fisher Scientific). The relative mRNA expression levels were then normalized by

Table 1: Primer sequence used for relative mRNA expression levels

Primer	Sequence
GAPDH	F: AATGGGCAGCCGTTAGGAAA
	R: GCCCAATACGACCAAATCAGAG
CTNNB1	F: GTAAAACGACGGCCAGTGGACTTCACCTGACAGATCCA
	R: CAGGAAACAGCTATGACCAGCTCATCATCCAGCTCCAG
APC	F: GACTCGGAAATGGGGTCCAA
	R: TCTTCAGTGCCTCAACTTGCT
LRP5	F: TTTTGGGTTACGCTGCTG
	R: AACTCTGTACCAGACGACCT
LRP6	F: AACGCGAGAAGGGAAGATGG
	R: CAAAGGGGCCGCTCTCAG

using the mRNA level of the reference gene (GAPDH) as an endogenous control in each sample. The mRNA data were analyzed using the comparative Ct method.

3 Results and discussion

3.1 Characterizations of green-synthesized *M. oleifera*-AgNPs

A color change from green to brown first indicated the synthesis of the green-synthesized *M. oleifera*-AgNPs that formed by reducing the silver ion, with the help of the reducing agents present in the *M. oleifera* leaf extract. The absorption peak was found at 380 nm of the UV-vis spectrum, as shown in Figure 1. The AgNPs

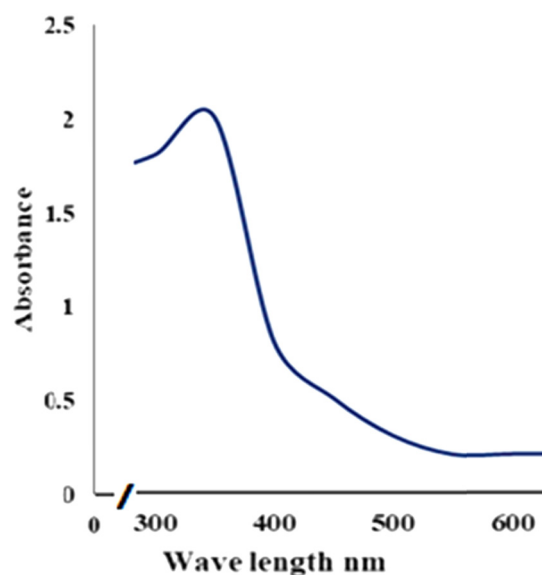


Figure 1: UV-vis spectra showing the absorbance peak of green-synthesized *M. oleifera*-AgNPs.

are the most interesting of all the metal NPs, due to silver's strong plasmonic interaction with light with sharply localized surface plasmon resonance (LSPR) bands [18]. The absorption peak position of AgNPs is in the range of 380–470 nm subjected to the size and shape of the particle [19].

The LSPR peak wavelength of AgNPs can be in the range from most visible to the near-infrared region, which can fluctuate by changing the shape, size, and dielectric environment of the NPs [20]. We use the aqueous extract of *M. oleifera* leaves as these leaves are very rich in protein which aids in bio-reducing of metal ions to nanoparticles. A leaf extract of *M. oleifera* is also very rich in phenolic compounds, flavonoids, and antioxidant-like vitamins C and A [21–23]. These compounds act as good reducing and capping agents to stabilize NPs and control their aggregates, once they are formed [24].

Figure 2 shows that the average size of green-synthesized *M. oleifera*-AgNPs, which is shown by dynamic

light scattering (DLS), was 197 nm, with a polydispersity index (Pdl) of 0.334. The average uniformity of an NP in a solution is estimated by the Pdl value, in that a larger value indicates a larger size distribution of NPs in a solution. The aggregation of NPs is also indicated by Pdl value since a sample is monodispersing if the Pdl value is less than 0.1 [25,26]. Thus, the values shown by DLS and Pdl in our results indicate little aggregation of NPs.

The TEM and SEM were used to gauge the surface morphology, size, and three-dimensional structure of green-synthesized *M. oleifera*-AgNPs, as shown in Figure 3. TEM shows an ultrathin image that indicates a two-dimensional structure, and SEM shows the three-dimensional structure of a material [27]. NPs were spherical with an average size of 25 nm, as shown by TEM images. Similar shapes were displayed using SEM images, but their sizes were in the range of 88.8–92 nm, which clearly shows aggregated, green-synthesized *M. oleifera*-AgNPs in the sample solution and agrees with DLS results. The

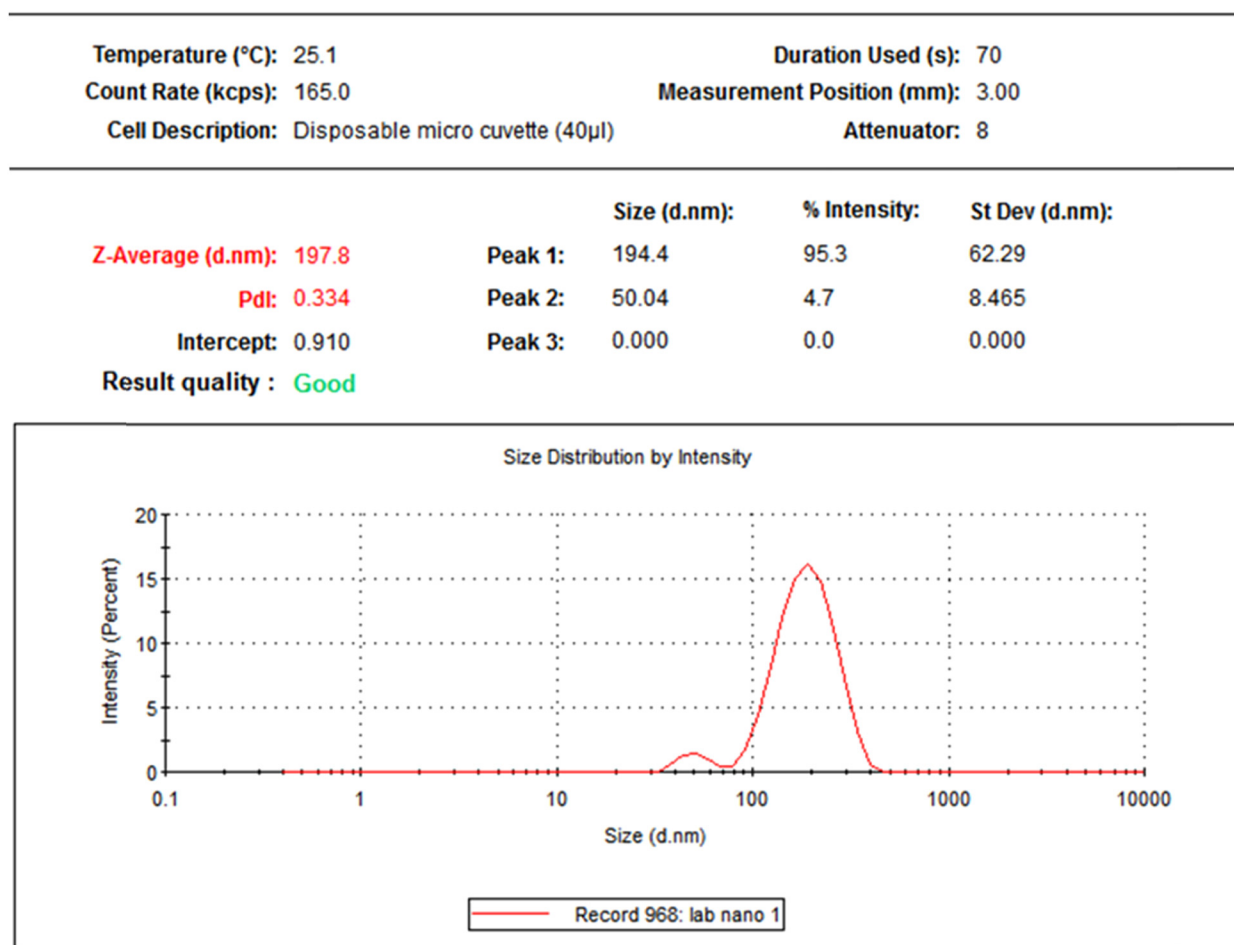


Figure 2: DLS result for the green-synthesized *M. oleifera*-AgNP.

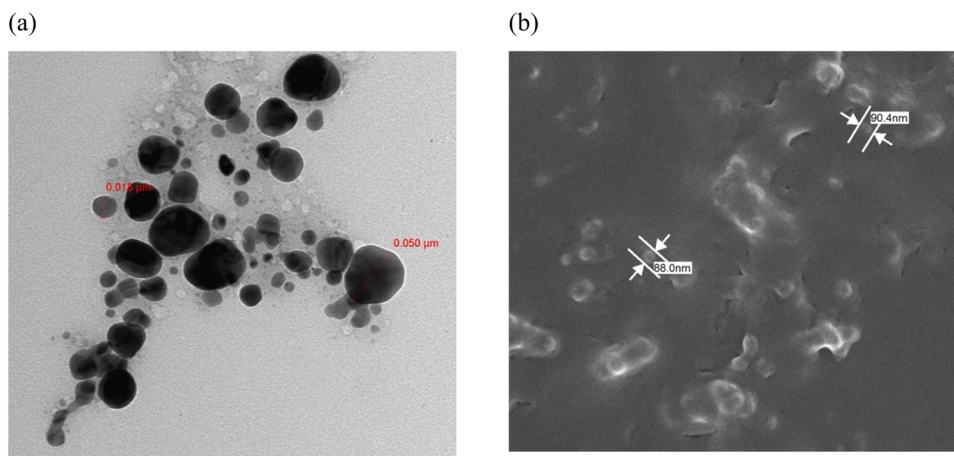


Figure 3: (a) TEM and (b) SEM micrographs of green-synthesized *M. oleifera*-AgNPs.

energy-dispersive spectrum (EDX) of the *M. oleifera*-AgNPs exhibited strong signals for potassium, silver, and the chlorine regions (Figure 4a shows the peaks visible on spectra, and Figure 4b shows the quantitative results).

3.2 Fourier transform infrared (FTIR) spectroscopy

FTIR spectroscopy was used to measure both the *M. oleifera* leaf extract and its reduced form, *M. oleifera*-AgNP solution, and to identify the changes in the bonds that may have occurred due to reduced silver ions and capped AgNPs. The amount of absorption peaks for both solutions is shown in Figure 5a and b. The 3,435, 2,359, and 1,634 cm^{-1} absorption peaks were assigned for the OH

bond of alcohols/phenols, the N-H bond of ammonium ions, and the N-H bond of amines, respectively, and were found in both solutions. Some additional readings were noted in the *M. oleifera*-AgNPs solution, such as the 1,394 cm^{-1} for the C-H bond of alkenes, 2,341 cm^{-1} for the C-C bond of terminal alkynes, and 456 cm^{-1} for the C-H deformation of alkynes. These results indicate that phenols and proteins play a major role in reducing silver ions to AgNPs [28].

3.3 Colon-cancer cell cytotoxicity

Both *M. oleifera* leaf extract and *M. oleifera*-AgNPs were tested for cytotoxicity against the HTC116 and SW480 human cancer cell lines by using an MTT assay, as shown

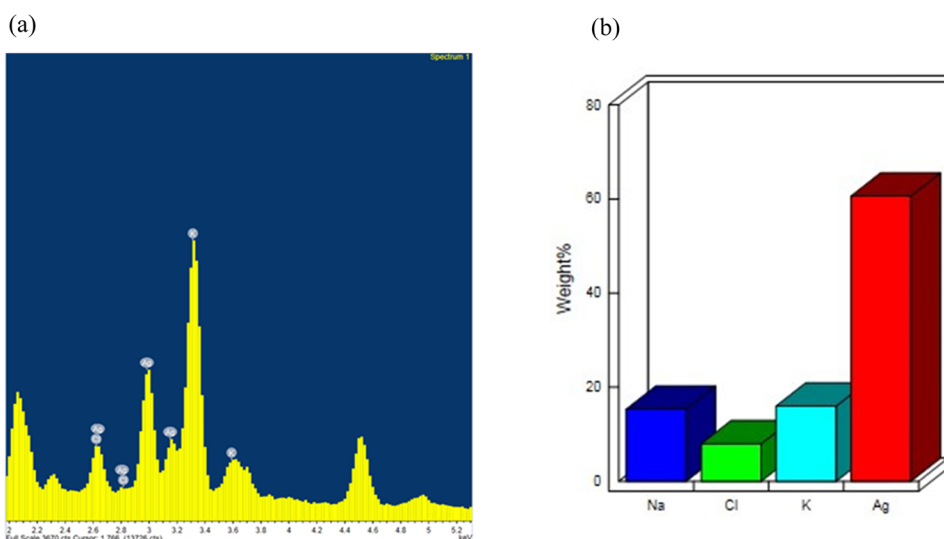


Figure 4: EDX elemental analysis of green-synthesized *M. oleifera*-AgNPs: (a) peaks visible on spectra, and (b) quantitative results.

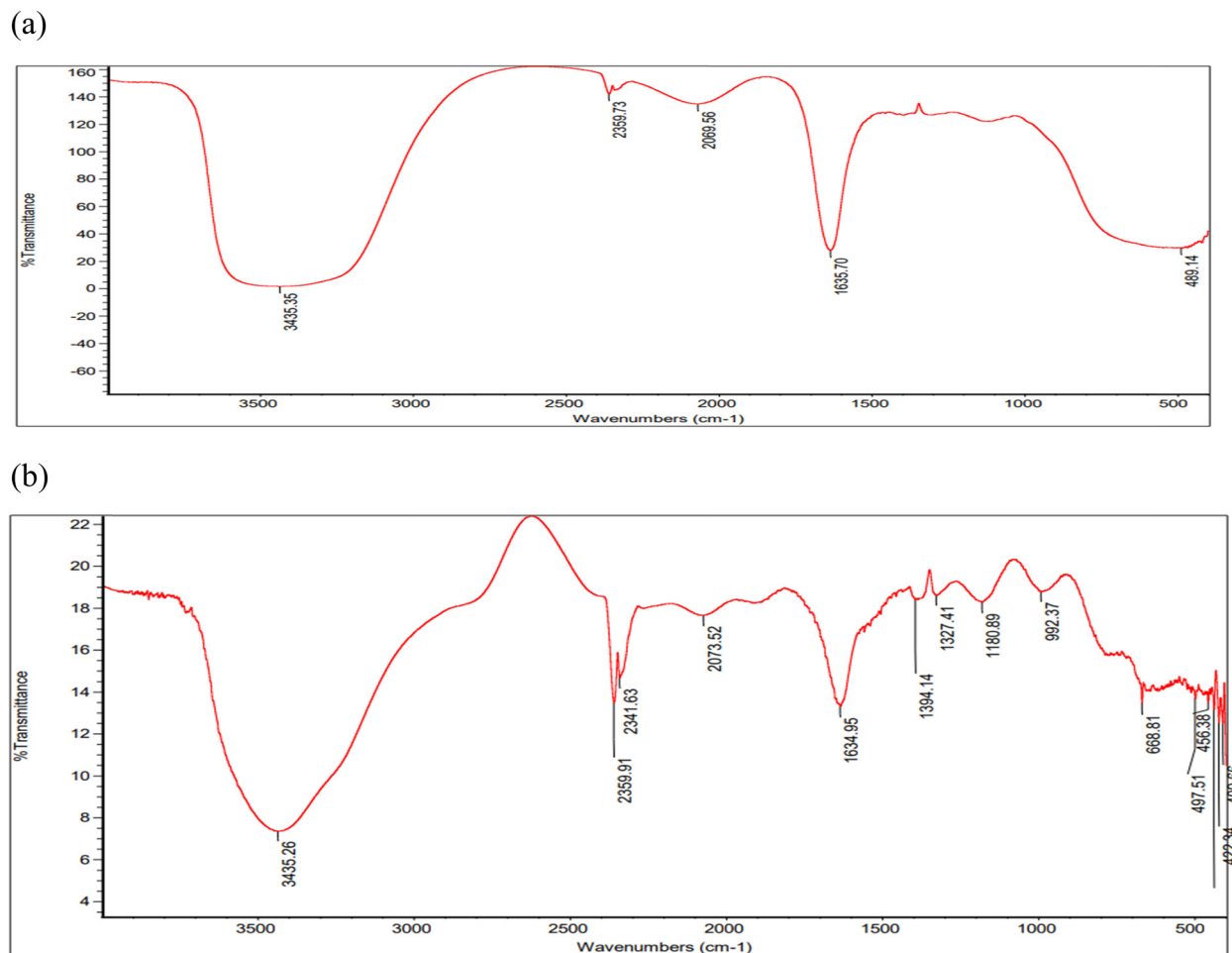


Figure 5: Infrared spectra of (a) *M. oleifera* leaf extract and (b) green-synthesized *M. oleifera*-AgNPs.

in Figure 6a and b. Both solutions decreased cell viability in a dose-dependent manner with an increased concentration from 3.12 to 100 $\mu\text{g}\cdot\text{mL}^{-1}$. *M. oleifera*-AgNP was found to be more cytotoxic than *M. oleifera* leaf extract at all concentrations. The IC_{50} recorded for *M. oleifera*-AgNP against HTC116 was 70 $\mu\text{g}\cdot\text{mL}^{-1}$ while SW480 recorded 100 $\mu\text{g}\cdot\text{mL}^{-1}$. Our results generally agree with many studies that highlight the efficacy of AgNPs against different types of cancer cell lines [7,29]. In the current study, the morphology of green-synthesized AgNPs was acceptable to reveal anticancer properties [29].

Green-synthesized AgNPs are used in many biomedical applications. AgNPs possess excellent antitumor potential by regulating the expression of many of the key genes that relate to numerous signaling pathways linked to oxidative stress, cell proliferation, DNA damage, and the cell-cycle arrest of cancer cells [30–32]. The Wnt/ β -catenin signaling pathway is altered in almost 90% of CRC patients, which makes it a critical therapeutic

target. Therapies that inhibit Wnt/ β -catenin signaling pathways are being performed in many clinical trials to monitor the response of patients, but chemoresistance is a major hurdle [33].

We examined the expression level of some key regulators of the Wnt/ β -catenin signaling pathway after treating the colon-cancer cell lines (HTC116 and SW480) with *M. oleifera* leaf extract and green-synthesized *M. oleifera*-AgNPs. These pathways play a major role in many biological processes, such as embryogenesis and tissue homeostasis; however, excessive activation of this pathway has been reported in most human malignancies, including CRC [34,35]. Almost 90% of CRC patients have mutations in some downstream components, such as adenomatous polyposis coli (APC) and β -catenin of the Wnt signaling pathway [36,37]. Also, mutations in the lipoprotein receptor-related proteins 5 and 6 (*LRP5/6*) coreceptors are detected in CRC patients frequently [38]. The *CTNNB1* and *APC* genes and *LRP5* and *LRP6* were included

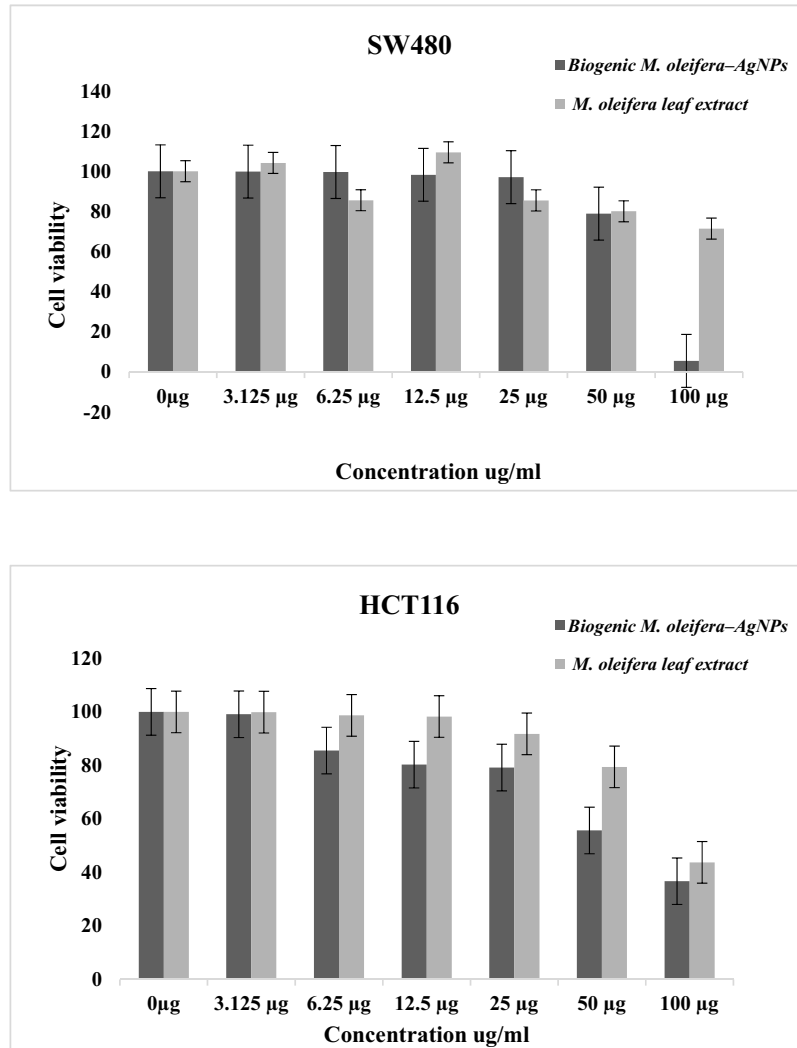


Figure 6: Cytotoxicity of *M. oleifera* leaf extract and green-synthesized *M. oleifera*-AgNPs on the SW480 and HCT116 human colon-cancer cell lines following 24 h exposure.

in the study. Figure 7 shows the gene-expression fold change in the control (without treatment) versus treated cell line.

The *APC* gene's expression decreased in cell line SW 480 for treatment with both leaf and green-synthesized AgNP extracts but was least effective in cell line HCT116. The mutant *APC* gene is expressed in SW480 while HCT116 expresses only wild-type *APC* [39]. Green-synthesized AgNPs decreased the expression of the *CTNNB1* gene remarkably, in both types of cell lines, as compared to leaf extract. This finding clearly indicates the inhibitory effect of green-synthesized AgNPs. The *LRP5* expression level was slightly increased in both cell lines after treatment with green-synthesized AgNPs. The *LRP5* gene expression can inhibit the tryptophan hydroxylase 1

expression level, which is the rate-limiting biosynthetic enzyme for serotonin [40]. Hence, *LRP5* can regulate the low expression of serotonin by downregulating tyrosine hydroxylase. Serotonin is known to promote CRC by modulating DNA repair and the immune response [41,42]. Our results confirm that increasing the expression level of the *LRP5* gene of green-synthesized AgNPs has anticancer potential. However, the expression level of the *LRP6* gene was remarkably decreased in treated cell lines. The low expression level of the *LRP6* gene has been linked to constrained cancer cell proliferation and delayed tumor growth in humans [43]. As a coreceptor for Wnt, the high expression of *LRP6* is associated with increased Wnt/ β -catenin signaling in colorectal adenocarcinomas [44].

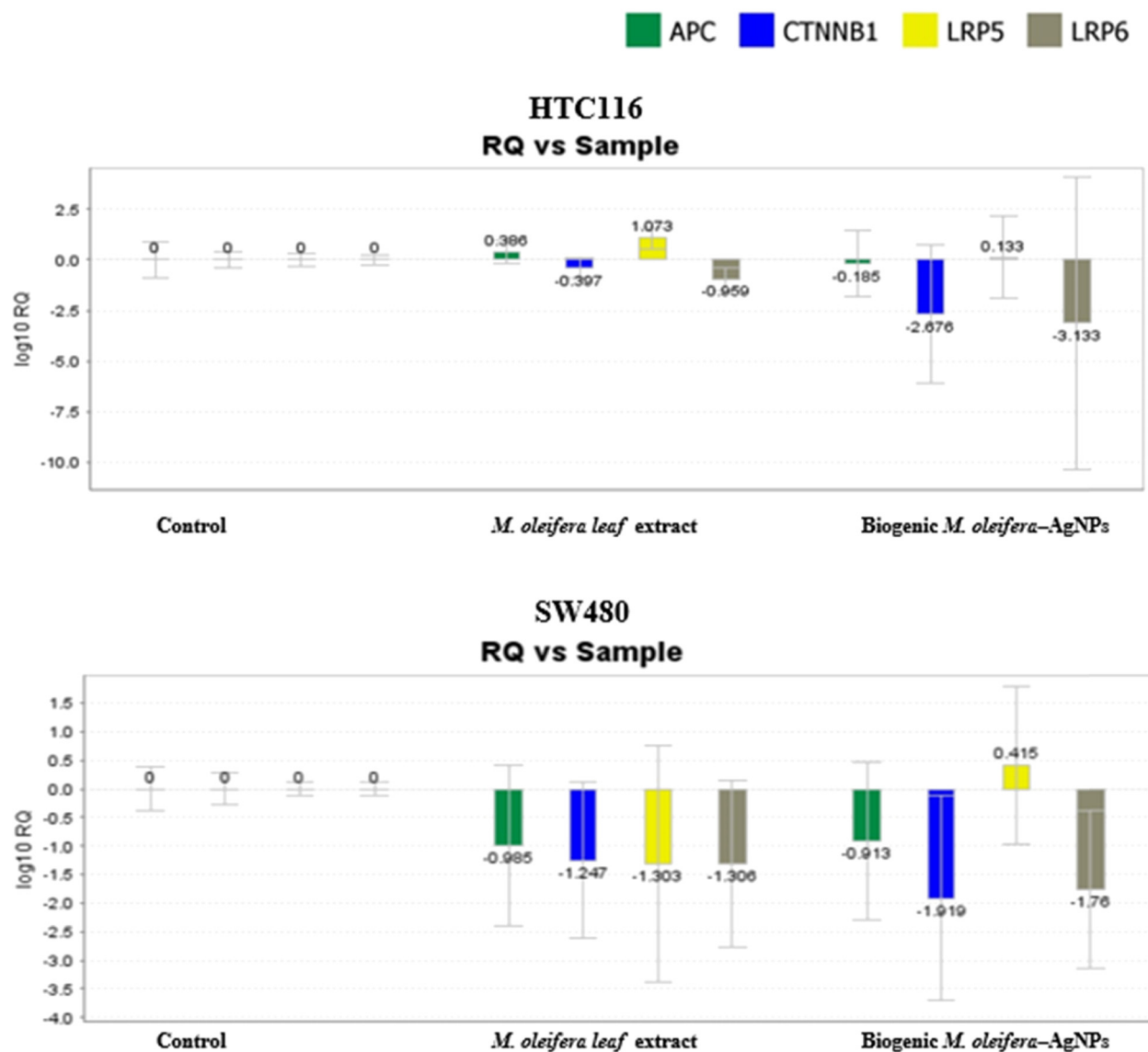


Figure 7: Gene expression in HTC116 and SW480 and cell lines treated with *M. oleifera* leaf extract and green-synthesized *M. oleifera*-AgNPs.

4 Conclusion

M. oleifera. leaf extract acts as a reducing and stabilizing agent for the green synthesis of AgNPs. At first, green-synthesized AgNPs were ascertained through the color change from green to brown with UV spectra absorption peak at 380 nm. *M. oleifera*-AgNPs were spherical in shape with an average size of 25 nm, which is acceptable to show potent anticancer activity against human cancer cell lines HTC116 and SW480. Further study is needed to explore its therapeutic effect by targeting Wnt/ β -catenin signaling pathways to overcome chemoresistance in patients.

Funding information: This research project was supported by Researchers Supporting Project no. RSP2022R495, King Saud University, Riyadh, Saudi Arabia.

Author contributions: Arwa Althomali: methodology; Maha H. Daghestani: project administration; Fatimah Basil Almukaynizi: methodology; Sabah Ahmed Al-Zahrani: methodology; Manal A. Awad: methodology; Nada M. Merghani: methodology; Wadha I. Bukhari: methodology; Eiman M. Ibrahim: methodology; Sherifah M. Alzahrani: methodology; Nouf Altowair: methodology; Afaf S. Al-Ghamd: methodology; Asma M. AlQahtani: methodology;

Rasha Ramadan, Ramesa Shafi Bhat: writing – original draft and data analysis.

Conflict of interest: Authors state no conflict of interest.

References

- [1] Alexander JW. History of the medical use of silver. *Surgical Infect.* 2009;10:289–92.
- [2] Midha K, Singh G, Nagpal M, Arora S. Potential application of silver nanoparticles in medicine. *Nanosci Nanotechnol.* 2016;6:82.
- [3] Qin Y. Silver-containing alginate fibres and dressings. *Int Wound J.* 2005;2:172–6.
- [4] Atiyeh BS, Costagliola M, Hayek SN, Dibo SA. Effect of silver on burn wound infection control and healing: review of the literature. *Burns: J Int Soc Burn Injuries.* 2007;33:139–48.
- [5] Lansdown AB. Silver in health care: antimicrobial effects and safety in use. *Curr Probl Dermatol.* 2006;33:17–34.
- [6] Zhang XF, Liu ZG, Shen W, Gurunathan S. Silver nanoparticles: synthesis, characterization, properties, applications, and therapeutic approaches. *Int J Mol Sci.* 2016;17:1534.
- [7] Daghestani M, Al Rashed SA, Bukhari W, Al-Ojayan B, Ibrahim EM, Al-Qahtani, et al. Bactericidal and cytotoxic properties of green synthesized nanosilver using *Rosmarinus officinalis* leaves. *Green Process Synth.* 2020;9:230–6.
- [8] Bhat RS, Almusallam J, Al Daihan S, Al-Dbass A. Biosynthesis of silver nanoparticles using *Azadirachta indica* leaves: characterisation and impact on *Staphylococcus aureus* growth and glutathione-S-transferase activity. *IET Nanobiotechnol.* 2019;13:498–502.
- [9] Mohammed Fayaz AM, Balaji K, Kalaichelvan PT, Venkatesan R. Fungal based synthesis of silver nanoparticles –an effect of temperature on the size of particles. *Colloids Surf B Biointerfaces.* 2009;74:123–6.
- [10] Al-Zahrani S, Astudillo-Calderón S, Pintos B, Pérez-Urria E, Manzanera JA, Martín L, et al. Green-synthesized silver nanoparticles with aqueous extract of green algae *Chaetomorpha ligustica* and its anticancer potential. *Green Process Synth.* 2021;10:711–21.
- [11] Niknejad F, Nabili M, Daie Ghazvini R, Moazeni M. Green synthesis of silver nanoparticles: advantages of the yeast *Saccharomyces cerevisiae* model. *Curr Med Mycol.* 2015;1:17–24.
- [12] Al-Zahrani SA, Bhat RS, Al-Onazi MA, Alwhibi MS, Soliman DA, Aljebrin, et al. Anticancer potential of biogenic silver nanoparticles using the stem extract of *Commiphora gileadensis* against human colon cancer cells. *Green Process Synth.* 2022;11:435–44.
- [13] Hussain I, Singh NB, Singh A, Singh H, Singh SC. Green synthesis of nanoparticles and its potential application. *Biotechnol Lett.* 2016;38:545–60.
- [14] Gliga AR, Skoglund S, Wallinder IO, Fadeel B, Karlsson HL. Size-dependent cytotoxicity of silver nanoparticles in human lung cells: the role of cellular uptake, agglomeration and Ag release. *Part Fibre Toxicol.* 2014;11:11.
- [15] Nallanthighal S, Chan C, Murray TM, Mosier AP, Cady NC, Reliene R. Differential effects of silver nanoparticles on DNA damage and DNA repair gene expression in Ogg1-deficient and wild type mice. *Nanotoxicology.* 2017;11:996–1011.
- [16] Xi Y, Xu P. Global colorectal cancer burden in 2020 and projections to 2040. *Transl Oncol.* 2020;14:101174.
- [17] Almatroudi A. The incidence rate of colorectal cancer in Saudi Arabia: an observational descriptive epidemiological analysis. *Int J Gen Med.* 2020;13:977–90.
- [18] Yguerabide J, Yguerabide EE. Light-scattering submicroscopic particles as highly fluorescent analogs and their use as tracer labels in clinical and biological applications. *Anal Biochem.* 1998;262:137–56.
- [19] Zaarour M, El Roz M, Dong B, Retoux R, Aad R, Cardin J, et al. Photochemical preparation of silver nanoparticles supported on zeolite crystals. *Langmuir Am Chem Soc.* 2014;30(21):6250–6.
- [20] Hermoso W, Alves TV, Oliveira CCC, Moriya EG, Ornellas FR, Camargo PHC. Triangular metal nanoprisms of Ag, Au, and Cu: modeling the influence of size, composition, and excitation wavelength on the optical properties. *Chem Phys.* 2013;423:142–50.
- [21] Vergara-Jimenez M, Almatrafi MM, Fernandez ML. Bioactive components in *Moringa oleifera* leaves protect against chronic disease. *Antioxidants.* 2017;6(16):91.
- [22] Nizioł-Łukaszewska Z, Furman-Toczek D, Bujak T, Wasilewski T, Hordyjewicz-Baran Z. *Moringa oleifera* L. Extracts as bioactive ingredients that increase safety of body wash cosmetics. *Dermatol Res Pract.* 2020;2020:8197902.
- [23] Özcan MM. *Moringa* spp: composition and bioactive properties. *South Afr J Bot.* 2020;129:25–31.
- [24] Marslin G, Siram K, Maqbool Q, Selvakesavan RK, Kruszka D, Kachlicki P, et al. Secondary metabolites in the green synthesis of metallic nanoparticles. *Materials.* 2018;11:940.
- [25] Clayton KN, Salameh JW, Wereley ST, Kinzer-Ursem TL. Physical characterization of nanoparticle size and surface modification using particle scattering diffusometry. *Biomicrofluidics.* 2016;10:054107.
- [26] Hughes JM, Budd PM, Grieve A, Dutta P, Tiede K, Lewis J. Polymerized high internal phase emulsion monoliths for the chromatographic separation of engineered nanoparticles. *J Appl Polym Sci.* 2014;132:41229.
- [27] Rauwel P, Siim K, Ferdov S, Erwan R. A review on the green synthesis of silver nanoparticles and their morphologies studied via TEM. *Adv Mater Sci Eng.* 2015;2015:1–9. <http://www.ncbi.nlm.nih.gov/pubmed/682749>.
- [28] El-Ansary A, Warsy A, Daghestani M, Merghani NM, Al-Dbass A, Bukhari W, et al. Characterization, antibacterial, and neurotoxic effect of green synthesized nanosilver using *Ziziphus spina Christi* aqueous leaf extract collected from Riyadh, Saudi Arabia. *Mater Res Exp.* 2018;5:025033.
- [29] Wang ZX, Chen CY, Wang Y, Li FXZ, Huang J, Luo ZW, et al. Ångstrom scale silver particles as a promising agent for low toxicity broad spectrum potent anticancer therapy. *Adv Funct Mater.* 2019;29:1808556. <http://www.ncbi.nlm.nih.gov/pubmed/1808556>.
- [30] Farah MA, Ali MA, Chen SM, Li Y, Al-Hemaid FM, Abou-Tarboush FM, et al. Silver nanoparticles synthesized from *Adenium obesum* leaf extract induced DNA damage, apoptosis

- and autophagy via generation of reactive oxygen species. *Colloids Surf B Biointerfaces*. 2016;141:158–69.
- [31] Mytych J, Zebrowski J, Lewinska A, Wnuk M. Prolonged effects of silver nanoparticles on p53/p21 pathway-mediated proliferation, DNA damage response, and methylation parameters in HT22 hippocampal neuronal cells. *Mol Neurobiol*. 2017;54:1285–300.
- [32] Yang T, Yao Q, Cao F, Liu Q, Liu B, Wang XH. Silver nanoparticles inhibit the function of hypoxia-inducible factor-1 and target genes: insight into the cytotoxicity and antiangiogenesis. *Int J Nanomed*. 2016;11:6679–92.
- [33] Yuan S, Tao F, Zhang X, Zhang Y, Sun X, Wu D. Role of Wnt/ β -catenin signaling in the chemoresistance modulation of colorectal cancer. *BioMed Res Int*. 2020;2020:9390878. doi: 10.1155/2020/9390878. PMC7109575. <http://www.ncbi.nlm.nih.gov/pubmed/32258160>.
- [34] van Neerven SM, Vermeulen L. The interplay between intrinsic and extrinsic Wnt signaling in controlling intestinal transformation. *Differ Res Biol Diversity*. 2019;108:17–23.
- [35] Nie X, Liu Y, Chen WD, Wang YD. Interplay of miRNAs and canonical Wnt signaling pathway in hepatocellular carcinoma. *Front Pharmacol*. 2018;9:657.
- [36] Cancer Genome Atlas Network. Comprehensive molecular characterization of human colon and rectal cancer. *Nature*. 2012;487:330–7.
- [37] Seshagiri S, Stawiski EW, Durinck S, Modrusan Z, Storm EE, Conboy CB, et al. Recurrent R-spondin fusions in colon cancer. *Nature*. 2012;488:660–4.
- [38] Eto T, Miyake K, Nosho K, Ohmuraya M, Imamura Y, Arima K, et al. Impact of loss-of-function mutations at the RNF43 locus on colorectal cancer development and progression. *J Pathol*. 2018;245:445–55.
- [39] El-Bahrawy M, Poulosom R, Rowan AJ, Tomlinson IT, Alison MR. Characterization of the E-cadherin/catenin complex in colorectal carcinoma cell lines. *Int J Exp Pathol*. 2004;85(2):65–74.
- [40] Walther DJ, Peter JU, Bader M. 7-Hydroxytryptophan, a novel, specific, cytotoxic agent for carcinoids and other serotonin-producing tumors. *Cancer*. 2002;94(12):3135–40.
- [41] Yadav VK, Ryu JH, Suda N, Tanaka KF, Gingrich JA, Schütz, et al. Lrp5 controls bone formation by inhibiting serotonin synthesis in the duodenum. *Cell*. 2008;135:825–37.
- [42] Kannen V, Bader M, Sakita JY, Uyemura SA, Squire JA. The dual role of serotonin in colorectal cancer. *Trends Endocrinol Metabolism: TEM*. 2020;31:611–25.
- [43] Raisch J, Côté-Biron A, Rivard N. A role for the WNT co-receptor LRP6 in pathogenesis and therapy of epithelial cancers. *Cancers*. 2019;11:1162.
- [44] Li Y, Lu W, He X, Schwartz AL, Bu G. LRP6 expression promotes cancer cell proliferation and tumorigenesis by altering β -catenin subcellular distribution. *Oncogene*. 2004;23:9129–35.